euspen's 15th International Conference & Exhibition, Leuven, Belgium, June 2015
www.euspen.eu

Theoretical study on the critical chip thickness in microcutting CaF_2 single crystals with crystal plasticity finite element method

Hao Wang*, Oltmann Riemer, Ekkard Brinksmeier

Laboratory for Precision Machining (LFM), University of Bremen, Badgasteiner Str. 2, Bremen 28359, Germany

*wang@uni-bremen.de; viccher@hotmail.com

Abstract
Substantial experimental work has been presented for microcutting calcium fluoride (CaF_2), aiming at devising the methodology for ductile-regime cutting of CaF_2 single crystals by means of quantifying the critical chip thickness. This paper establishes the theoretical understanding of the dominant factor for the variation in the critical chip thickness in relation to crystallographic orientations, and contributes to modelling of the microcutting process using crystal plasticity finite element method (CPFEM).

Keywords: critical chip thickness, calcium fluoride, crystal plasticity, finite element method, microcutting

1. Introduction

CaF_2 is one of the key materials for high power optics, and is ideal for optical applications (λ=0.15 µm - 9 µm). In spite of conventional processing methods for CaF_2 like pitch polishing and magneto-rheological finishing (MRF), recent experimental study has taken the advantages of ultraprecision diamond turning technology for fabrication of complex optical geometries. Critical problems and the-state-of-the-art research of microcutting brittle crystalline materials are summarised in table 1. Although numerical methods have been developed for deformation simulation of crystalline materials, hitherto, no model has been proposed for the theoretical study of CaF_2 microcutting. To fill the blank in research, this paper integrates crystal plasticity constitutive model into the FEM framework, whereby the key problem of determining the critical chip thickness is addressed in light of material anisotropy.

Table 1. Key problems in cutting brittle crystalline materials

Research area	Problem and solution
Ductile-regime cutting of brittle materials	Key problems: - crack and subsurface damage [1] - critical chip thickness [2, 3]. Experimental methods: plunge [4] and fly cutting [5], scratching [6], diamond turning [3]; Numerical methods: analytic model [7], molecular dynamics simulation [8]
Material anisotropy effect	Periodic undulation of machined surface [9], micro-cutting force variation [10], chip morphology and tool vibration [11]
Modelling	Tensile loading [12], CaF_2 indentation [13]

2. Development of the CPFEM simulation

A 3D orthogonal microcutting model was set up using the commercial FEM software ABAQUS/Standard v6.11. The CaF_2 workpiece with a dimension of 0.02 mm × 0.01 mm × 0.001 mm was meshed by 9,601 eight-node linear brick (C3D8R) elements. A rigid analytical surface was employed to model the diamond tool. A well-lubrication (i.e. frictionless) condition was assumed for the rigid-deformable body interaction. Due to the short cutting time, heat generation was not considered. In all the simulations, constant depth of cut of 1 µm and cutting speed of 0.01 mm/s were adopted. The simulation of orthogonal cutting was performed on (111) plane and in five crystallographic directions as shown in figure 1. No subsequent crack damage was addressed by the CPFEM simulation herein based on the assumption of ductile-regime cutting.

Crystal plasticity constitutive equations for CaF_2 were programmed into ABAQUS through the user subroutine UMAT, following a similar procedure previously devised for another commercial FEM software MSC.Marc [14]. Assuming crystallographic slip governed by Schmid's law was the sole cause of plastic deformation, plastic shear rate $\dot{\mathbf{F}}^{\mathbf{p}}$ was expressed by slip rate $\dot{\gamma}^{(\alpha)}$ of the slip system α, where $\mathbf{s}$ and $\mathbf{n}$ were the slip direction and the normal of slip plane in Eq. (1).

$$\dot{\mathbf{F}}^{\mathbf{p}} = \sum_{\alpha} \dot{\gamma}^{(\alpha)} \mathbf{s}^{(\alpha)} \otimes \mathbf{n}^{(\alpha)} \mathbf{F}^{\mathbf{p}} \quad (1)$$

The slip rate was determined by the critical resolved shear stress $\tau_c^{(\alpha)}$, rate sensitivity factor m, and strain hardening factor $h_{\alpha\beta}$, following Eqs. (2)-(4).

$$\dot{\gamma}^{(\alpha)} = \dot{\gamma}_0^{(\alpha)} \left| \tau^{(\alpha)} / \tau_c^{(\alpha)} \right|^{1/m} \operatorname{sgn}\left(\tau^{(\alpha)}\right) \quad (2)$$

$$\dot{\tau}_c^{(\alpha)} = \sum_{\beta} h_{\alpha\beta} \left| \dot{\gamma}^{(\beta)} \right| \quad (3)$$

$$h_{\alpha\beta} = q_{\alpha\beta} \cdot h_0 \left(1 - \tau_c^{(\beta)} / \tau_s\right)^a \quad (4)$$

CaF_2 possesses six slip systems of {100} <110> at ambient temperature. Its elastic stiffness constants C_{11}, C_{12}, and C_{44} are 168.16 GPa, 48.54 GPa, and 33.81 GPa, respectively. The reference slip rate $\dot{\gamma}_0^{(\alpha)}$ and rate sensitivity factor m were experimentally determined as 0.001 s^{-1} and 0.05, with the initial shear strength and self-hardening coefficient of 110 MPa and 100 MPa for (111) plane microcutting [13].

3. Results and discussion

Figure 1 shows the simulation results of Mises stress with the initial chip formation in cutting along the five selected crystallographic directions on the (111) plane. Taking account of crystal anisotropy, the opposing side views of the deformed work material are shown for the stress contour. For clear presentation, cutting tools are removed from these plots.

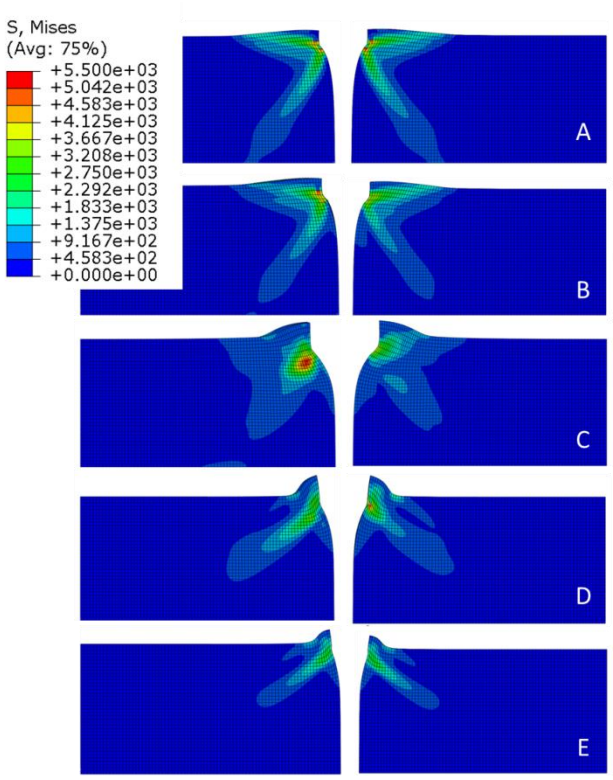

Figure 1. Simulated Mises stress on (111) plane with cutting directions of (A) $[\bar{1}\,\bar{1}\,2]$, (B) $[\bar{1}\,\bar{2}3]$, (C) $[0\,\bar{1}\,1]$, (D) $[1\bar{3}2]$, and (E) $[1\bar{2}1]$

The most significant anisotropy exhibits in cutting along $[0\,\bar{1}\,1]$ direction. Stress distribution helps categorise cutting of CaF_2 single crystals into two distinct types on the (111) plane: type I – with stress concentration spreading from tool tip to bulk material which is nearly perpendicular to primary deformation zone (PDZ) as shown in figures 1A, 1B, 1D, and 1E; and type II – with confined stress concentration within PDZ as shown in figure 1C. Unless microcrack can be effectively suppressed in the immediate vicinity of cutting edge (inelastic zone), type I stress will unavoidably foment macrocrack initiated from the microcrack cluster [15], and cause subsurface damage in greater depths [16]. On the contrary, type II stress is not as catastrophic, since it does not contribute sufficient driving force for crack propagation. This also theoretically explains why a large critical chip thickness was experimentally established for direction $[0\,\bar{1}\,1]$; whilst about merely one sixth of the thickness was identified for the other four directions (refer to figure 2). Furthermore, the stress states applied on the cleavage plane (111) of CaF_2 also favour the cutting direction $[0\,\bar{1}\,1]$. Compared to the other four crystallographic directions, cutting in $[0\,\bar{1}\,1]$ direction imposes tensile stress (in red colour) only within the PDZ in front of the advancing tool and compressive stress (in green colour) below the inelastic zone (figure 3B); however, cutting in the $[\bar{1}\,\bar{1}\,2]$ direction (figure 3A) causes tensile stress in a much wider volume.

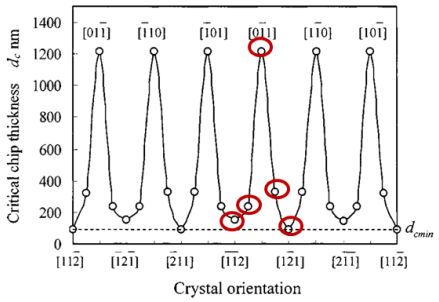

Figure 2. Experimental results of the critical chip thickness with regard to different crystallographic directions: the corresponding directions of (A)-(E) in figure 1 are marked by the red circles from left to right in the reproduced figure from the work by Yan *et al.* [3]

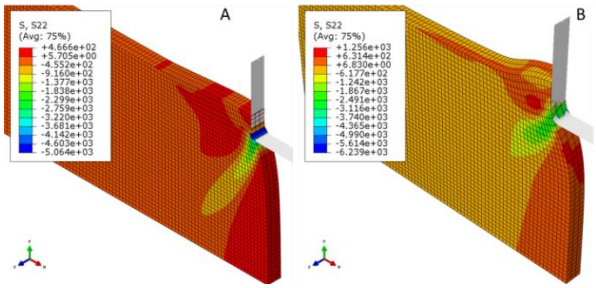

Figure 3. Stress contours on the CaF_2 cleavage plane (111) in cutting along the crystallographic directions of (A) $[\bar{1}\,\bar{1}\,2]$ and (B) $[0\,\bar{1}\,1]$

4. Conclusions

This paper develops a crystal plasticity finite element model for CaF_2 microcutting. The theoretical study reveals the effect of material anisotropy on stress distribution in the primary deformation zone and subsurface, which elucidates the mechanism of the variation in critical chip thickness for different crystallographic directions on the (111) plane of CaF_2 single crystals. This work not only contributes to the numerical modelling methodology, but also furthers the understanding on the microcutting process of brittle materials.

Acknowledgements

The authors gratefully appreciate the financial support from Alexander von Humboldt Foundation.

References

[1] Yan J, Asami T, Harada H and Kuriyagawa T 2012 *CIRP Ann.-Manuf. Techn.* **64** 131-4
[2] Blake P N and Scattergood R O 1990 *J. Am. Ceram. Soc.* **73** 949-57
[3] Yan J, Syoji K and Tamaki J 2004 *J. Vac. Sci. Technol.* B **22** 46-51
[4] Fang F Z and Venkatesh V C 1998 *CIRP Ann.-Manuf. Techn.* **47** 45
[5] O'Connor B P, Marsh E R and Couey J A 2005 *Precis. Eng.* **29** 124-32
[6] Patten J A, Gao W and Yasuto K 2005 *J. Manuf. Sci. E.-T. ASME* **127** 522-32
[7] Bifano T G, Dow T A and Scattergood R O 1991 *J. Eng. Ind.-T. ASME* **113** 184-9
[8] Cai M B, Li X P and Rahman M 2007 *Int. J. Mach. Tool. Manu.* **47** 75-80
[9] Marsh E R, John B P, Couey J A, Wang J, Grejda R D and Vallance R R 2005 *J. Vac. Sci. Technol.* B **23** 84-9
[10] Lee W B, Cheung C F and To S 2002 *J. Manuf. Sci. E.* **124** 170-7
[11] Wang H, To S, Chan C Y, Cheung C F and Lee W B 2011 *Int. J. Mach. Tool. Manu.* **51** 512-9
[12] Peirce D, Asaro R J and Needleman A 1982 *Acta Metall.* **30** 1087
[13] Zhang Q and Lambropoulos J C 2007 *J. Appl. Phys*. **101** 043105
[14] Lee W B, Wang H, Chan C Y and To S 2013 *Int. J. Mach. Tool. Manu.* **75** 82-6
[15] Zhang B, Tokura H and Yoshikawa M 1988 *J. Mater. Sci.* **23** 3214-24
[16] Tan Y, Yang D and Sheng Y 2009 *J. Eur. Ceram. Soc.* **29** 1029-37